Path effects and local elastic site amplification: two case studies on Mt Etna (Italy) and Vega Baja (SE Spain)

Luciano Scarfi [1]

Horst Langer [1]

Mariano Garcia-Fernandez [2]

Maria-Jose Jimenez [2,*]

Email: mj.jimenez@csic.es

[1] Istituto Nazionale di Geofisica e Vulcanologia – Osservatorio Etneo, Catania, Italy

[2] MNCN, CSIC, Madrid, Spain

Abstract

Local site effects, normally ground motion amplification, represent one of the main components when developing ground motion simulations and play an important role in the potential earthquake damage. In the framework of the UPStrat-MAFA project a stochastic finite-fault simulation method was selected for the generation of synthetic ground motion scenarios. This method uses spectral site correction functions to account for site amplification effects. These local effects may undergo significant changes due to the source–receiver configuration (i.e., distance, source depth and ray incidence). This holds in particular for reflection and transmission coefficients which may strongly vary depending on the source–receiver geometry, and may alter the characteristics of the spectral site-correction functions. A strategy is proposed to account for local site effects in the context of the regional geological structure, considering SH-waves propagating in a 1D velocity model. Spectral correction functions are derived by comparing Green's functions obtained for general velocity models and those more detailed at shallow depths. The developed approach is applied in two of the test areas selected in the project, the Mt Etna in Italy and the Vega Baja in SE Spain. The results show the different behaviour in two environments, i.e., volcanic and tectonic, with different seismicity characteristics, and highlight the importance of performing specific site-effect studies in some regions where standard building code soil factors could have some limitations to evaluate the potential for ground motion amplification.

Keywords

~~Site effect~~
~~Amplification~~
Path effects
Site amplification
Mt Etna
Italy
Vega Baja
Spain

1. Introduction

Local site effects are known to play an important role in the potential damage caused by an earthquake. In standard seismic building codes constant soil factors by ground type are used to define elastic response spectra, e.g., for representing the seismic action. In most codes, ground types account for the uppermost part of the stratigraphic column (e.g., 30 m in the EC8) as geotechnical parameters can be obtained with a limited effort. More detailed scenarios on ground motion and controlling parameters can be obtained by the creation of synthetic scenarios. In the framework of the UPStrat-MAFA project synthetic scenarios were created using the EXSIM code (see Motazedian and Atkinson 2005; Boore 2009). Besides ~~parameters regarding~~ the seismic source and whole path wave propagation effects, site amplification parameters—such as the geotechnical characteristics of the shallow layers, topographic effects, non-linear behavior of the material— are an important issue for the assessment of ground shaking during relevant earthquakes and are therefore intensively studied.

Amplitude amplification of weak material at the surface depends on the impedance structure of the rock underneath. Often a soil profile is given up to the "engineering bedrock", i.e., the layer best suited to support building foundations ~~to a depth~~ where Vs reaches values of around ~~750~~ 400–800 m/s (Satoh et al. 1995; Kinoshita 2007; García-Fernández and Jiménez 2012).

However, the focus of the seismic source is typically situated in hard rock—"seismic bedrock"—where Vs is considerably higher. This amplification is not necessarily constant for all relevant events. It may undergo significant changes due to the source–receiver configuration. This holds in particular for reflection and transmission coefficients which may strongly vary depending on the source–receiver geometry.

We devote specific attention to this geometrical effects, accounting for the possible characteristics of the material underneath the shallow layers. For the sake of simplicity we limit ourselves to SH-waves propagating in a 1D model. In practice this simple model is often considered as a valid first order approximation for the description of site effects. We neglect 2D/3D effects which may become important in conditions met in deep mountain valleys (see Bard and Bouchon 1985) but are less critical at our example sites. We focus on two test areas: the Mt Etna volcano (Siciliy, Italy) and the Vega Baja region (SE Spain). Information on the subsurface geological structure on Mt Etna has been made available by numerous geotechnical logs, allowing the compilation of a map of impedance and soil classification in the sense of the EC8. In the Vega Baja area, the properties of the surface material have been investigated through systematic analysis of available geological and geotechnical data, and H/V analysis, which again were used to derive 1D velocity models for the assessment of site effects (García-Fernández and Jiménez 2012).

AQ1

2. Geometry dependence of reflection and transmission in 1D models

The problem of site effect and its dependence on the source–receiver geometry and the interaction of deeper and shallow layers can be easily illustrated considering the simple case of one layer over a half space. Suppose a solid–solid layer boundary, and a plane SH wave incident from medium 1 to medium 2. The reflection coefficient is given by

$$R_{11} = \rho_1\beta_1 \cos\alpha_1 - \rho_2\beta_2 \cos\alpha_2 / \rho_1\beta_1 \cos\alpha_1 + \rho_2\beta_2 \cos\alpha_2 \quad (1)$$

and the transmission coefficient by

$$T_{12} = 1 + R_{11}. \quad (2)$$

ρ_1, β_1, are the density and shear wave velocity of medium 1, ρ_2, β_2 the corresponding parameters of medium 2. α_1 and α_2 are the angles of the reflected and transmitted wave, both measured against vertical. With $\beta_1 > \beta_2$, R_{11} decreases with the angle α_1, consequently also T_{12} decreases as the ray incidence becomes more shallow. In the case of vertical incidence we have the maximum of both the reflection coefficient

$$R_{11} = \rho_1\beta_1 - \rho_2\beta_2 / \rho_1\beta_1 + \rho_2\beta_2 \quad (3)$$

and the transmission coefficient

$$T_{12} = 1 + R_{11} = 2\rho_1\beta_1 / \rho_1\beta_1 + \rho_2\beta_2 \quad (4)$$

Consider a single layer overlying a half space. Using Haskell matrices for SH waves (Haskell 1953, 1960) we find the ratio of incident amplitude A_1 and observed amplitude at the surface A_S

$$A_S/A_1 = 2\rho_1\beta_1 \cos\alpha_1 / \rho_2\beta_2 \cos\alpha_2 \quad (5)$$

for frequencies with constructive interference. The factor 2 is due to the free surface amplification. Again we obtain a maximum for steep incidence, i.e., $\alpha_1 = \alpha_s = 0$.

In realistic models reflection and refraction will be more complicated, as impedance contrasts will exist both above and below the source and 2D/3D effects may be present. In practice we have no clues about the details of 2D or 3D layer boundaries and we limit ourselves to 1D velocity structures. For this case we may use efficient approaches for the calculation of Green's functions, such as the reflectivity method by Müller (1985), which has been used here.

3. The Mt Etna region

The seismicity in the area reveals a quite particular pattern. Besides strong, but rare events caused by the regional tectonic activity, the area is often hit by small but shallow earthquakes, causing frequently heavy damage around the epicenter because of the foci falling close to earth's surface. Especially the shallow seismicity brings along peculiarities with respect to wave propagation. First, given the shallow depth, ray incidence angles vary rapidly with distance from the epicenters. As shown above we must be aware of the fact that soil amplification may strongly vary with distance. A second issue is the position of the foci, which fall in depth where sedimentary material is present. In the context of the simulation with EXSIM we therefore account for this by choosing model parameters, in particular the seismic velocity for the layer hosting the source as well as for the assessment of the source scaling laws. Besides, the particular circumstances on Mt Etna must be accounted for also for the

assessment of site correction functions (Fig. 1).

In order to highlight the problem we start from a shallow velocity model obtained from a multichannel analysis of surface waves at the accelerometer station CAT (Fig. 1). The station is of specific interest as it is the only one for which strong motion records of the October 29, 2002 San Bongiardo earthquake (M = 4.8, I_{EMS} = VIII) are available. The records were intensively discussed in Milana et al. (2008) for their particular spectral characteristics. The velocity model for the shallow structure can be found in the Italian Accelerometric Archive (ITACA) data base (http://itaca.mi.ingv.it; Luzi et al. 2008; Pacor et al. 2011; see also Langer et al. 2015). The model reports the shallow velocity structure down to the engineering bedrock, which is reported at a depth of 60–65 m. The model for the deeper layers is obtained from an educated guess using the information available in the literature, as described in detail in Langer et al. (2015). We assume the presence of shale and marnes below the engineering bedrock. From the literature (see Schön 1983) we obtain first an estimate for the *P* wave velocities of this materials. For this type of rock *P* wave velocities are reported to strongly depend on pressure. Once obtained the *P* wave structure we convert to shear velocities following essentially Castagna et al. (1985) ~~(Fig. 1)~~.

Fig. 1

At the *top*, a simplified tectonic map with the location of the Mt. Etna area. *Green triangle* indicates the location of station CAT. At the *bottom*, a sketch profile of Mt Etna (from Branca et al. 2011) is shown. The edifice of Mt Etna is made up of basaltic material, composed of solid rock but also less competetent tuffitic material. The thickness of the volcanogenic material reaches about 2 km at the center of the volcano and decreases towards it margins. To the south thick sediments consisting of marls and sands are encountered, with low shear wave velocities

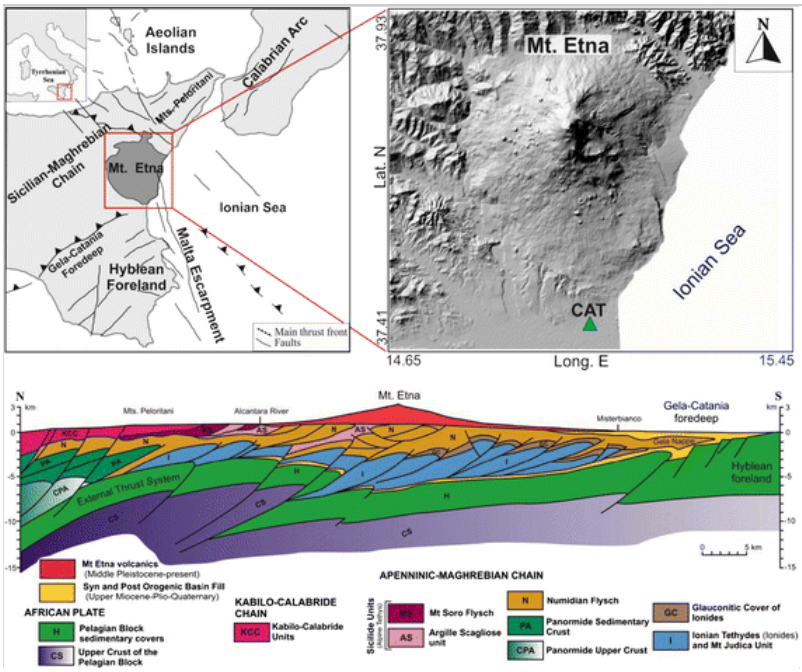

The EXSIM code allows for two spectral correction functions, one is a “crustal amplification function” and a second one, is referred to as “site amplification function”. One could be tempted to account for propagation effects occurring between the source and the bedrock layer using the crustal amplification function, whereas the specific site effects were accounted for by the site amplification function. This way, the two functions act as two—independent—filters in chain. This, however, is questionable from ~~form~~ a theoretical point of view, as the effects encountered in the upper layers strongly depend on the impedance structure found below, and vice versa. To bypass these theoretical shortcomings we therefore apply a strategy for the assessment of the site correction function which was already applied in Langer et al. (2015). We reconsider the site CAT mentioned in that paper. The assessment of the correction for this site starts from the model shown in Fig. 2. As noticed earlier, synthetic simulations with the EXSIM code have to account for the specific conditions of shallow foci. Therefore, in the standard simulation for shallow Mt Etna events Langer et al. (2015) used a shear-wave velocity of V_s = 1.8 km/s for the source area volume, whereas the value used in the geometrical spreading term was 2.4 km/s up to a distance of 40 km. The standard simulation is considered to represent velocity structures equivalent to the red curve in Fig. 2, with a homogeneous velocity in the layers above the source. In other words, we assume that propagation effects of this model are already fixed by properly choosing the whole-path attenuation parameters—essentially Q, and the parameters controlling geometrical spreading $1/(4\pi\rho V_s^3)$, with ρ being the density.

Fig. 2

Velocity model derived for the site CAT. The *blue line*, which includes the detailed shallow structure, goes up to 1.5 km, the usual focal depth in Mt Etna area; while the *red dotted line* represents a reference model with homogeneous velocity for the layer above the seismic source region (see also Langer et al. 2015)

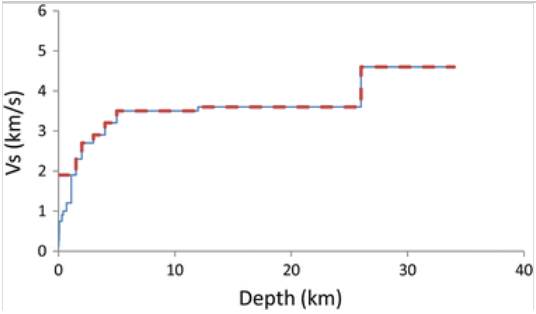

AQ2

In EXSIM we use the spectral correction functions (crustal and site) when we wish to account for the effects of a specific shallow velocity structure. In our strategy we define in particular the site correction function in order to allow for the amplification effects which were not accounted for using the standard parameters of whole path attenuation in EXSIM. In order to assess these lacking effects we calculate the spectral representation of theoretical Green's functions. The first one is obtained for the reference model (red curve in Fig. 2), which should represent the path effects in the standard EXSIM simulations. The source is located at a depth of 1.5 km, and the uppermost layers in this model have the same parameters as the layers where the source is found. The second one is calculated including the shallow layers at CAT (blue curve in Fig. 2). These Green's functions were obtained using the reflectivity method (Müller 1985). The spectral ratios of the Green's functions for the two models are shown in Fig. 3. Each curve corresponds to a specific source–receiver geometry. Keeping fixed the focal depth at 1.5 km, we increase the epicentral distance from 1 to 50 km. Forming the ratios of spectra we get a measure of effects introduced by the shallow low velocity layers, which were not accounted for by the afore mentioned whole path attenuation parameters.

Fig. 3

Ratio of the spectra of Green's functions for the two velocity models defined at site CAT (Fig. 2) for different epicentral distances and a focal depth of 1.5 km

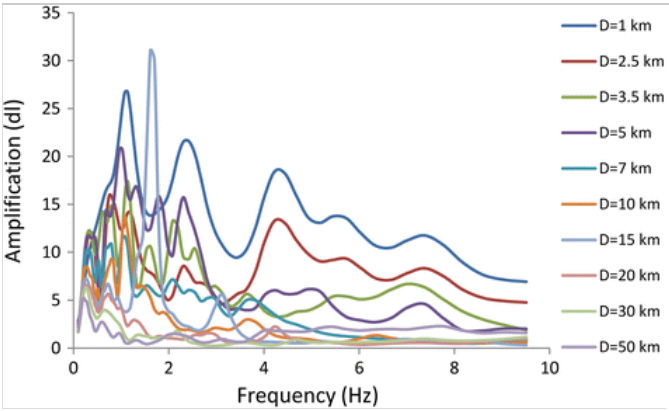

In Fig. 4 we present synthetic decay curves for PGA, one using a flat site correction function (marked as PGA_H) and one applying the site correction functions shown in Fig. 3. Figure 4a shows the results for a source similar to the S. Bongiardo earthquake (M4.8, and stress parameter 20 bar). Figure 4b represents a typical shallow event on Mt Etna (M3.3, and 5 bar; see Langer et al. 2015). In both cases we notice a strong amplification close to the epicenter, with a factor near 10. The amplification decreases with distance. In the weak motion case of Fig. 4b it almost vanishes at distances larger than 30 km.

Fig. 4

Decay of PGA with epicentral distance for **(a)** a source with M4.8 and 20 bar (similar to the 2002 S. Bongiardo earthquake), and **(b)** a small shallow earthquake (M3.3 and 5 bar). Source and whole-path attenuation parameters are the same as used in Langer et al. (2015)

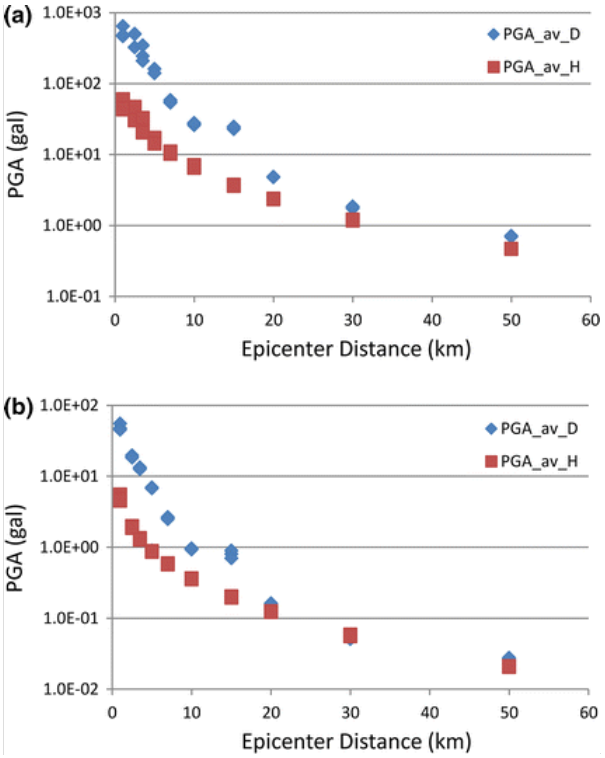

4. Vega Baja area (SE Spain)

The Vega Baja is located in the lower course of the Segura River or Lower Segura Basin (LSB), in SE Spain (Fig. 5). The LSB is one of the Neogene-Quaternary depressions developed in the Betic Cordillera in SE Iberian Peninsula. Materials of Tertiary and Mesozoic age from the External Betics unit form, in general, the basement rocks. The basin fill is post-orogenic comprising materials from the Miocene up to Holocene (Montenat 1977; Silva et al. 1993; Alfaro et al. 2002a, b). Detailed characterization of the soils in the Vega Baja has been carried out by García-Fernández and Jiménez (2012), using H/V results from ambient-noise surveys. It was shown that low-to-medium consistency and relative density materials, forming the most superficial soils, can reach significant thickness, around 50 m, at relatively broad areas in the northern and western parts of the region. Also, in most of the central and western parts this soils overlay a relatively thick layer (around 30–260 m) of sedimentary rocks, which correspond to the engineering bedrock in the area (V_S around 400–600 m/s).

Fig. 5

Location and geotechnical model of the Vega Baja area. *Dots* identify the location of ambient-noise recording sites. *Red dots* Reliable data to derive 1D soil models. (Modified from García-Fernández and Jiménez 2012)

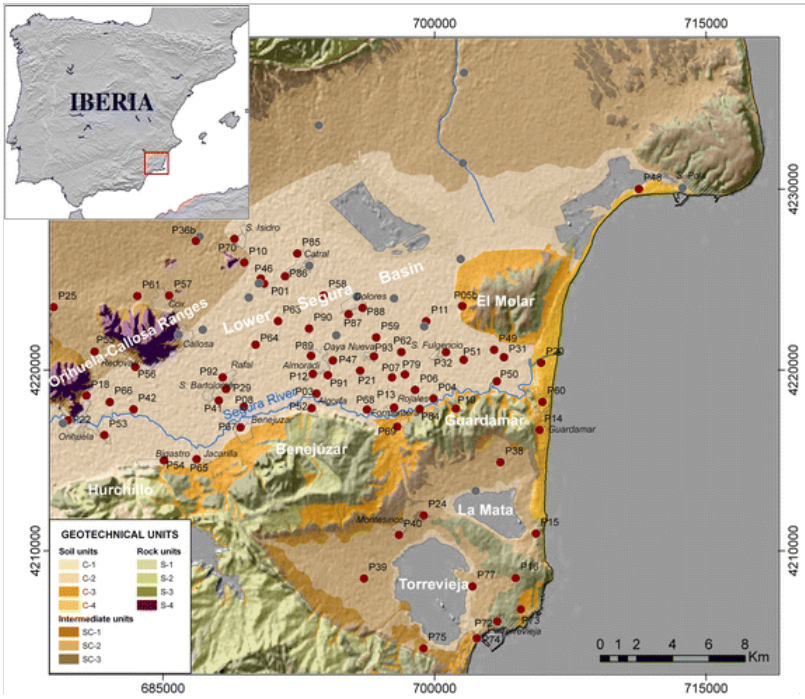

Following a similar strategy as in Mt Etna, we selected an average model representative of the local subsurface structure down

to the engineering bedrock (Fig. 6), as obtained by the 1D inversion of H/V results (García-Fernández and Jiménez 2012). We used regional information (Carbonell et al. 1998) to model the velocity structure for the intermediate parts of the crust, i.e., the medium between the shallow layers and the seismic source region (Fig. 6). Contrary to the situation met at Mt Etna, foci in SE Spain are deeper, mostly located at 5–10 km depth. For this application we have assumed an average focal depth of 5 km, and a representative site located in the area. This results in weaker distance-dependence site amplification, though still visible (Fig. 7). In the inset of Fig. 7 the amplification is averaged over various frequency ranges. Only foci at epicentral distances of the order of focal depth or lower (corresponding to high incident angles) show different amplification (larger) for most frequencies. In this case, the use of a single soil factor over all distances brings some error but still is a suitable compromise between simplicity and accuracy.

Fig. 6

Velocity model for the Vega Baja area. *Blue line* Shallow average model from García-Fernández and Jiménez (2012). *Red dotted line* Regional average model from Carbonell et al. (1998)

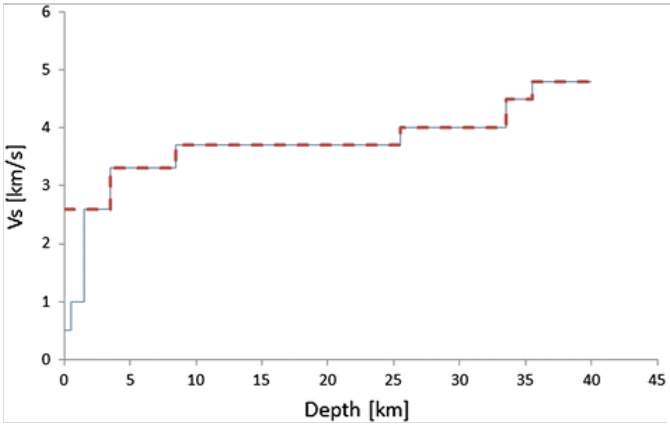

Fig. 7

Ratio of the spectra of Green's functions for the two velocity models defined in the Vega Baja (Fig. 6) for different epicentral distances and a focal depth of 5 km. The *inset panel* shows mean corrections considering various frequency ranges

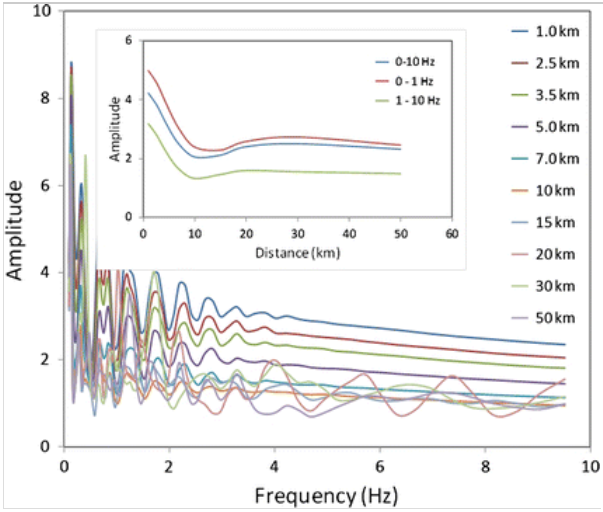

Again, similar to Mt Etna region, we made EXSIM simulations to obtain the synthetic decay curves for PGA in Fig. 8, for a typical small event (M3.5 and 250 bar), and a larger one, with M5.2 and 150 bar ~~(Fig. 8 a, b, respectively)~~. In both cases, significant amplification only appears very close to the epicenter, at distances less than 10 km.

Fig. 8

Decay of PGA with epicentral distance for **(a)** an earthquake with M5.2 and 150 bar, and **(b)** a typical small earthquake (M3.5 and 250 bar)

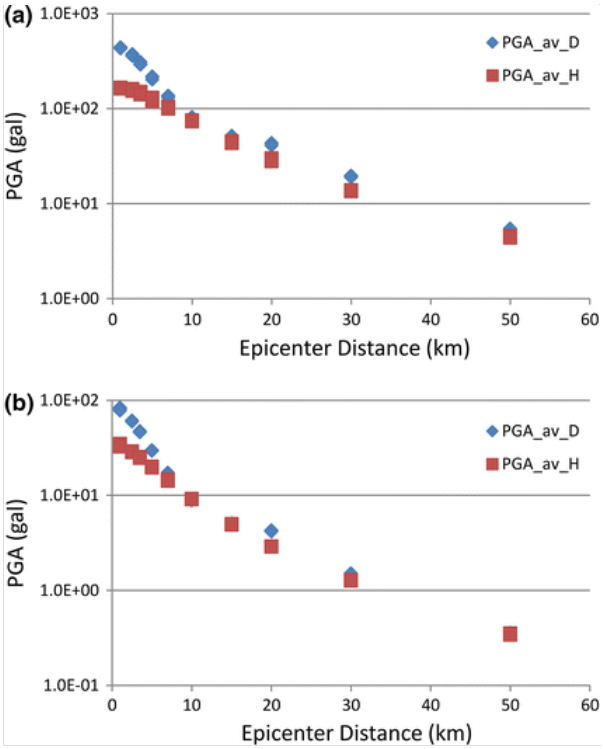

5. Conclusions

Site effects, usually amplification, represent a main issue for the estimation of earthquake ground motion. Besides topographic effects and non-linear behavior of materials, amplitude amplification due to the presence of impedance contrasts is a key factor in hazard studies. This work ~~short note~~ focuses on site-amplification effects in terms of visco-elastic behavior of propagation medium.

Most seismic building codes use specific soil factors by ground type to define elastic response spectra. The ground types are defined based on the average shear wave velocity in the first 30 m below the surface. However, site amplification could also depends on the ground properties at depth as well as in the source–receiver geometry. In our study we carried out synthetic simulations for two test areas of the UPSTRAT-MAFA project, i.e., Mt. Etna (Italy) and the Vega Baja (SE Spain). A strategy is proposed to account for local site effects in the context of the regional geological structure. We derived spectral correction functions by comparing Green's functions obtained for general velocity models and those more detailed at shallow depths.

Simulation of ground motions (peak ground acceleration) for the two model types reveals the strongest amplification for sites closer to the epicenter. In the Vega-Baja the obtained amplification effects are only noticeable at very short epicentral distances (less than 10 km), while at Mt Etna remains significant up to around 20 km, mostly due to the very shallow events in the area (1.5 km depth) in comparison with shallow depths (5–10 km) in the Vega Baja, and amplification is larger. The use of building code soil factors could work in Vega Baja but for sites very close to the epicenter. In Mt Etna, on the contrary, using code soil factors could be questionable, and specific site analysis would be advisable.

Acknowledgments

This research was developed in the framework of the European project UPStrat-MAFA (Grant Agreement 230301/2011/613486 /SUB/A5). Part of the work was supported by the Spanish projects CGL2007-62454, and CGL2010-11831-E. We used the Generic Mapping Tools (GMT) version 5.1.1 by Wessel et al. (2013) for the maps. The authors are grateful for the helpful comments and suggestions from the reviewers.

References

Alfaro P, Andreu M, Delgado JM, Estévez A, Soria JM, Teixidó T (2002a) Quaternary deformation of the Bajo Segura blind fault (eastern Betic Cordillera, Spain) revealed by high-resolution reflection profiling. Geol Mag 139(3):331–341

Alfaro P, Delgado J, Estévez A, Soria JM, Yébenes A (2002b) Onshore and offshore compressional tectonics in the eastern Betic Cordillera (SE Spain). Mar Geol 186:337–349

Bard PY, Bouchon M (1985) The two-dimensional resonance of sediment-filled valleys. Bull Seism Soc Am 75: 519-541.

Boore DM (2009) Comparing stochastic point-source and finite-source ground-motion simulations: SMSIM and EXSIM.

Bull Seism Soc Am 99:3202–3216

Branca S, Coltelli M, Groppelli G, Lentini F (2011) Geological map of Etna volcano, 1:50,000 scale. Ital J Geosci 130(3):265–291. doi:10.3301/IJG.2011.15

Carbonell R, Sallares V, Pous J, Dañobeitia JJ, Queralt P, Ledo JJ, García Dueñas V (1998) A multidisciplinary geophysical study in the Betic chain (southern Iberia Peninsula). Tectonophysics 288:137–152

Castagna JP, Batzle ML, Eastwood RL (1985) Relationship between compressional wave and shear wave velocities in clastic silicate rocks. Geophysics V 50:571–581

García-Fernández M, Jiménez MJ (2012) Site characterization in the Vega Baja, SE Spain, using ambient-noise H/V analysis. Bull Earthq Eng 10(4):1163–1191

Gresta S, Langer H (2002) Assessment of seismic potential in South eastern Sicily. In: Brebbia CA (ed) Risk analysis, III. WIT Press, Southampton, pp 617–626

AQ3

Haskell NA (1953) The dispersion of surface waves in layered media. Bull Seism Soc Am 43:17–34

Haskell NA (1960) Crustal reflection of plane SH-waves. J Geophys Res 65:4147–4150

Kinoshita S (2007) Propagation characteristics of bedrock waves traveling from pre-Tertiary basement to engineering bedrock. Earth Planets Space 59:1173–1179

Langer H, Tusa G, Scarfì L, Azzaro R (2015) Ground-motion scenarios on Mt Etna inferred from empirical relations and synthetic simulations. Bull Earth Eng. doi:10.1007/s10518-015-9823-1

Lentini F, Carbone S, Guarnieri P (2006) Collisional and postcollisional tectonics of the Apenninic–Maghrebian orogen (southern Italy). In: Dilek Y, Pavlides S (eds) Postcollisional tectonics and magmatism in the Mediterranean region and Asia, vol 409. GSA Special Paper, pp 57–81

AQ4

Luzi L, Hailemikael S, Bindi D, Pacor F, Mele F, Sabetta F (2008) ITACA (ITalian ACcelerometric Archive): a Web Portal for the Dissemination of Italian Strong-motion Data. Seismol Res Lett 79(5):716–722. doi:10.1785/gssrl.79.5.716

Milana G, Rovelli A, De Sortis A, Calderoni G, Coco G, Corrao M, Marsan P (2008) The role of long-period ground motions on magnitude and damage of volcanic earthquakes on the Mt. Etna, Italy. Bull Seism Soc Am 98:2724–2738. doi:10.1785/0120080072

Montenat C (1977) Les basins néogènes et quaternaries du Levant d'Alicante à Murcie (Cordillères Bétiques orientales, Espagne), Stratigraphie, paléontologie et evolution dynamique. Doc Lab Géol Univ Lyon 69:345

Motazedian D, Atkinson GM (2005) Stochastic finite-fault modeling based on a dynamic corner frequency. Bull Seism Soc Am 95:995–1010

Müller G (1985) The reflectivity method: a tutorial. J Geophys 58:153–174

Pacor F, Paolucci R, Luzi L, Sabetta F, Spinelli A, Gorini A, Nicoletti M, Marcucci S, Filippi L, Dolce M (2011) Overview of the Italian strong motion database ITACA 1.0. Bull Earth Eng 9:1723–1739. doi:10.1007/s10518-011-9327-6

Satoh T, Kawase H, Sato T (1995) Evaluation of local site effects and their removal from borehole records observed in the Sendai region, Japan. Bull Seismol Soc Am 85:1770–1789

Schön J (1983) Petrophysik. Enke, Stuttgart, p 405

Silva PG, Goy JL, Somoza L, Zazo C, Bardají T (1993) Landscape response to strike-slip faulting linked to collisional settings: quaternary tectonics and basin formation in the Eastern Betics, southestern Spain. Tectonophysics 224:203–289

Wessel P, Smith WHF, Scharroo R, Luis JF, Wobbe F (2013) Generic mapping tools: improved version released. EOS Trans AGU 94:409–410